Journal of Ceramic Processing Research. Vol. 13, No. 4, pp. 437~440 (2012)

J O U R N A L O F
Ceramic Processing Research

Sonochemical synthesis of hydroxyapatite and fluoroapatite nanosized bioceramics

Faranak Barandehfard, Mansoor Keyanpour-Rad, Azarmidokht Hosseinnia, Seyed Mohammad Kazemzadeh, Mohammad Reza Vaezi and Amir Hassanjani-Roshan*

Division of Nanotechnology and Advanced Materials, Materials and Energy Research Center (MERC), Tehran, Iran

Synthesis of hydroxyapatite (HA) and fluoroapatite (FA) nanoparticles were carried out via a simple sonochemical technique. For this purpose, diammonium hydrogen phosphate [$(NH_4)_2HPO_4$], hydrated calcium nitrate [$Ca(NO_3)_2.4H_2O$], and ammonium fluoride [NH_4F] were used as the precursors for preparation of the nanosized bioceramics. The sonochemical process was carried out at 50 W and a temperature of 30 °C, while the pH of the reactions was kept above 10. The HA and FA nanoparticles were calcined at 600 and 700 °C. The samples were completely crystalline at the latter calcinations temperature. Both of the nanoparticles were characterized by Fourier transform infrared spectroscopy (FT-IR), X-ray diffraction (XRD)\, scanning electron microscopy (SEM) and transmission electron microscopy (TEM). These analyses demonstrated that the particle were crystalline having sizes approximately in the range of 30-60 nm. It was also found that the nanoparticles were spherical and semispherical in shape.

Key words: Sonochemical synthesis, Nanoparticles, Bioceramics, Hydroxyapatite, Fluoroapatite.

Introduction

Bioceramics such as hydroxyapatite and fluoroapatite are suggested as perfect mineral substitutes for bone reconstruction in orthopedic and dentistry due to their excellent biological behavior, biocompatibility to hard tissue and bioactivity [1-3]. The hydroxyapatite (HA) crystal structure is similar to the natural apatite in the human skeletal system. These bioceramics are considered as calcium phosphate complexes. Stoichiometric formulas of HA and FA are ($Ca_{10}(PO_4)_6(OH)_2$) and ($Ca_{10}(PO_4)_6F_2$) [2], respectively. It is observed that HA and FA are present in bone and teeth in the form of nanometre sized crystals [4]. Therefore, extensive research to prepare these nano-sized particles with appropriate stoichiometry, high purity and crystallinity have been undertaken. A number of methods have been tried to prepare nano-sized HA and FA powders, such as spray drying [5], wet chemistry [6], sol-gel [7-9], chemical precipitation [8, 10], microemulsion technique [11], a mechanochemical [12-14], electrodeposition [15], solvothermal approach [16], hydrothermal treatment [16, 17] and sonochemical synthesis [18]. Control of morphology and the mean size of the powders are important in different applications of HA and FA. The stoichiometry and purity of the powders also affect the properties of such particles in many application fields, such as the orthopedic and dentistry fields in the form of paste, granules, or porous blocks for implants [3]. Recently, HA has been used for a variety of biomedical applications and tissue engineering fields, such as implant coating and matrics for drug release control [7]. Also, HA nanoparticles have been successfully applied in various fields such as sensors, catalysts and the water purification industry. In recent years, attention has been paid to the sonochemical route of synthesis of hydroxyapatite, because of its simplicity and low cost [18-22].

In this research, by taking advantage of the sonochemical method HA and FA nanoparticles were synthesized. Different calcination temperatures were selected to obtain the most crystalline and smaller size nanoparticles. The structures and morphologies of the nanoparticles were also evaluated by different methods of analysis, such as TG-DTA, FTIR, XRD, SEM and TEM.

Experimental

Materials and equipments

All the chemicals were of analytical grades and applied as received from Merck Chemical Company. Hydrated calcium nitrate, diammonium hydrogen phosphate, ammonium fluoride, absolute ethanol and ammonium hydroxide were used as the precursors for the preparation of the nanomaterials.

A high-intensity ultrasonic probe (Misonix S4000, Ti horn, 20 kHz, 500 W/cm^2, USA) and a flat-bottomed Pyrex glass vessel (total volume of 100 ml) were used for the ultrasound irradiation reactor.

Preparation of nanosized HA and FA via the sonochemical process

In the presence of the ultrasonic probe, an aqueous

*Corresponding author:
Tel : +98-263-6204130
Fax: +98-263-6201888
E-mail: Amir_Hassanjani@yahoo.com

Table 1. The sonication experimental conditions

Sample	Initial power (W)	Ultrasonic intensity (W/cm^2)	Reaction temperature (°C)	Reaction time (h)	pH
HA	40	~40	30	2	10
FA	50	~50	30	2	10

solution of 50 mmol of diammonium hydrogen phosphate in 50 ml distilled water was added dropwise to a solution of 84 mmol hydrated calcium nitrate in 50 ml absolute ethanol.

Similar to the above procedure, FA nanoparticles were synthesized. For this purpose the mixture of aqueous solutions of diammonium hydrogen phosphate (50 mmol in 45 ml distilled water) and ammonium fluoride (16.7 mmol in 5 ml distilled water) were added to the ethanoloic solution of hydrated calcium nitrate (84 mmol in 50 ml absolute ethanol).

In both of the syntheses, it was observed that the color of the slurry mixture in both procedures gradually changed from colorless before the reaction to white-lactic after the reaction was completed, which was the sign of HA and FA formation. In the experiments,the initial power of the sonicator was set at 50 W, while maintaining the temperature at 30 °C (see Table 1). It was important to control the pH of the reaction mixture during the experiment so as not to decrease to below 10 and if so, a few dropes of NH_4OH solution were added. The resulting precipitates in both experiments were centrifuged, collected, washed by absolute ethanol three times, dried at 80 °C for 5 h and crushed by a laboratory mortar and pestle to obtain the fine powders. Both HA and FA powders were then calcined at 300 °C at rate of 10 $Kminute^{-1}$ and held at this temperature for 1 h. Each of the powders after calcinius at 300 °C was divided into 2 parts namely (b) and (c) and the former was re-calcinated at 600 °C and the latter 700 °C for 1 h (the heating rate was 10 $Kminute^{-1}$), respectively.

Characterization

The evaluation of crystal structure and the size were performed by an X-ray diffractometer (Philips PW 3710, Netherlands-Holland), using Cu $K\alpha_1$ radiation ($\lambda = 1.54\ A^{\circ}$). All samples were examined in the 2θ range from 20-60 ° at a scanning speed of 0.04 ° 2θminute^{-1} and a step size of 0.02 ° and step time of 0.5 s. The XRD analysis was done on both powders before and after the calcination steps.

FT-IR (VECTOR 33 FT-IR spectrometer, Bruker Germany, KBr pellet) was used to determine the chemical structure of the nanoparticles. The wavelength range was 4000-400 cm^{-1} at 4 cm^{-1} resolution averaging 45 numbers of scans.

Thermogravimetry and differential thermal analysis were studied by simultaneous thermal analysis (STA; simultaneous thermal analysis). A thermoanalyzer (STA; PL 1640, England), with start heating from room temperature up to 1200 °C with the rate of 10 $Kminute^{-1}$.

The morphology of the samples was determined, using transmission and scanning electron microscopy (TEM; ZEISS, Germany and SEM; VEGA\\ TESCAN Czech Republic). TEM samples were prepared by dispersing a few drops of HA and FA on carbon films supported by copper grids, and SEM samples were prepared by a dispersing thin layer of the powders on aluminum grids while the surface of each specimen was coated with a thin layer of gold before SEM examination. The SEM analysis was performed at 15 kV. Particle size measurements were carried out by using an Able Image Analyzer v3.6.

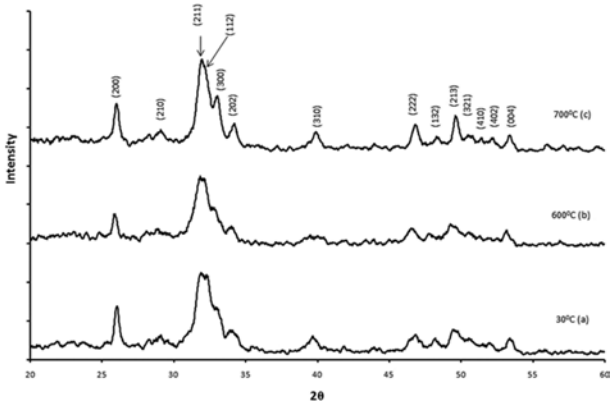

Fig. 1. XRD patterns of HA nanoparticles (a) 30 °C, the synthesis temperature, (b) 600 °C and (c) 700 °C.

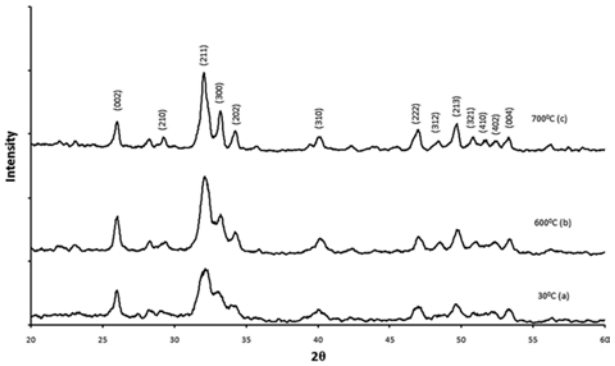

Fig. 2. XRD patterns of FA nanoparticles at (a) the synthesis temperature (30 °C), (b) 600 °C and (c) 700 °C.

Results and discussion

X-Ray diffraction analysis

The X-Ray diffraction patterns of the nanoparticles are shown in Figs. 1 and 2. Fig. 1a and 2a show the X-ray diffraction patterns of HA and FA samples obtained at 30 °C(a) while the calcined samples of both of these bioceramics at 600 °C(b) and 700 °C(c) are shown in Fig. 1b, 2b and 1c, 2c, respectively. Checking with the related card of the pure materials, it was confirmed that the nanoparticles were formed in almost pure states (JCPDS card, HA: 00-001-1008

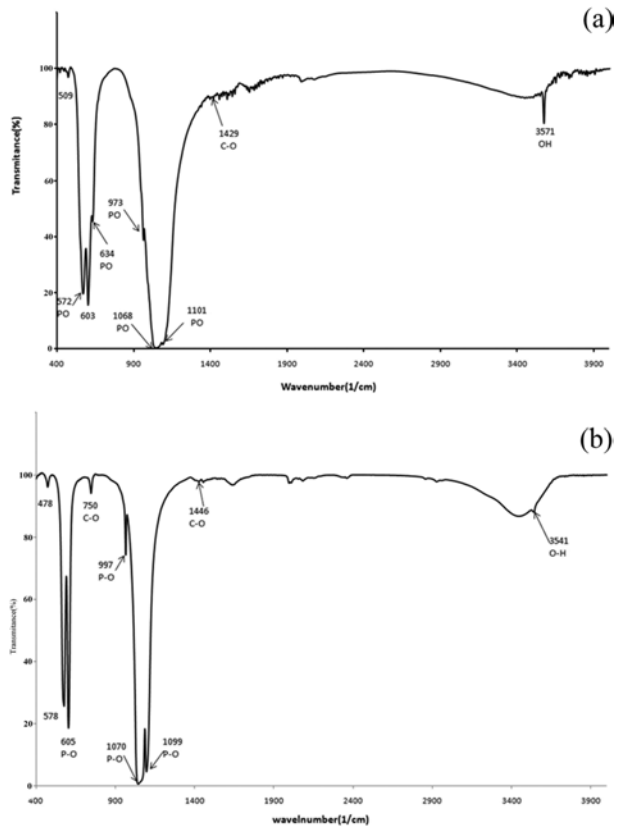

Fig. 3. FTIR spectra of the nanopowders (a) HA (b) FA nanopowders calcined at 700 °C.

and FA: 00-003-0736). The peaks of HA at (211) and (112) are merged together in the XRD patterns of FA due to fluorination. In addition, the XRD pattern of FA demonstrated that it has formed at a higher degree of crystallinity than HA, which is due to the presence of fluorine in the structure [23]. It is noticed from Figs1 and 2 that the samples were formed as a mixture of amorphous and crystalline compounds and gradually change to completly crystalline nanoparticles at 700 °C. Therefore, SEM, TEM and FTIR analyses were carried out on HA and FA nanoparticles which were calcined at 700 °C.

FTIR analysis

The FTIR spectra of HA and FA nanoparticles are shown in Fig. 3a and 3b. As may be seen in the spectra, the OH stretching vibrations of HA and FA appear at 3571 and 3541 cm^{-1}, respectively. The bands at 1101, 1068, 973 cm^{-1} are due to the phosphate stretching vibrations of HA, while for FA nanoparticles these bands appears at 1099, 1070 and 997 cm^{-1}. The phosphate bending vibrations of HA appeared at 603, 572 and 509 cm^{-1} and bands at 605, 578 and 478 cm^{-1} are the characteristic of the phosphate bending vibrations of FA. The small bands at 1429 and 1446 cm^{-1} in the spectra correspond to the atmospheric CO_2 of the air in HA and FA samples, respectively [23]. It was noticed that the intensity of the band at

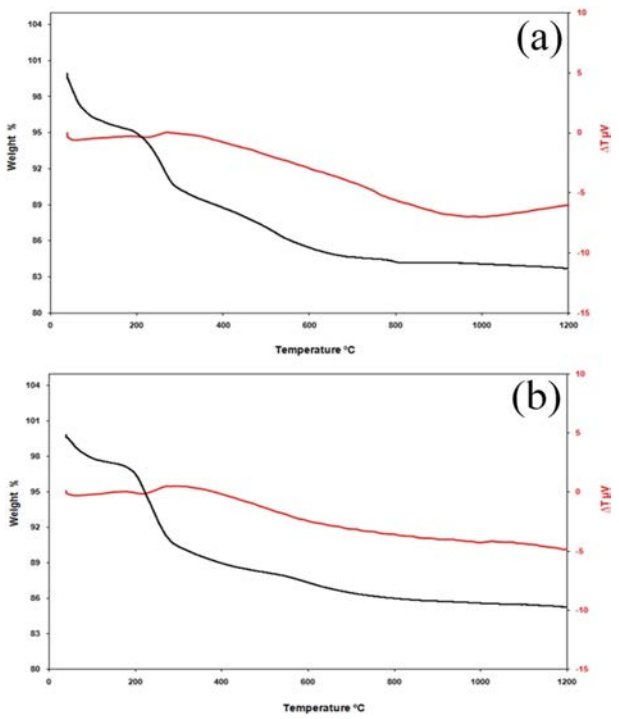

Fig. 4. TG-DTA curves of the (a) HA and (b) FA nanoparticles.

3571 cm^{-1} gradually decreased, while the band at 634 cm^{-1} completely disappeared, confirming the formation of FA nanoparticles.

TG and DTA analysis

The TG and DTA analysis were carried out in the range of 25-1200 °C under atmospheric air. The DTA and TGA curves for HA and FA nanoparticles are illustrated in Fig. 4a and b. According to Fig. 4a, the first endothermic region from 200 °C to 300 °C, with a peak at about 250 °C, corresponds to the dehydration of the precipitating complex and the loss of physical adsorbed water molecules in the powders. With an increase in the temperature from 25 °C to 1200 °C no peak has been observed, except a weight loss of 15% in the TGA curve which is assumed to be the result of gradual dehydroxylation of HA powders [10]. Also, Fig. 4b shows that a crystallization temperature peak at around 250 °C. The TG-DTA curve shows that the loss of FA powders is about 14%. The weight loss remains constant while the DTA curve decreases with an increase in the temperature because this weight loss depends on the intrinsic value of the material and is realized in a special temperature range and is independent of an increase in the temperature.

SEM analysis

SEM images of the samples are shown in Fig. 5a and b. These images depict that the morphology of all of the HA and FA nano powders after calcination at 700 °C were spherical and semispherical. Also it was shown that the particle size of both nanopowders were approximately in the range of 30-60 nm. It was also

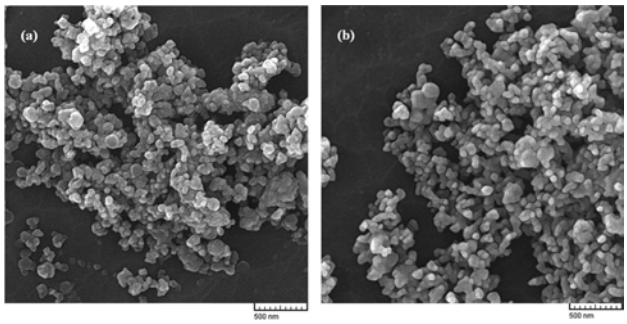

Fig. 5. SEM images of (a) HA and (b) FA nanopowders calcined at 700 °C.

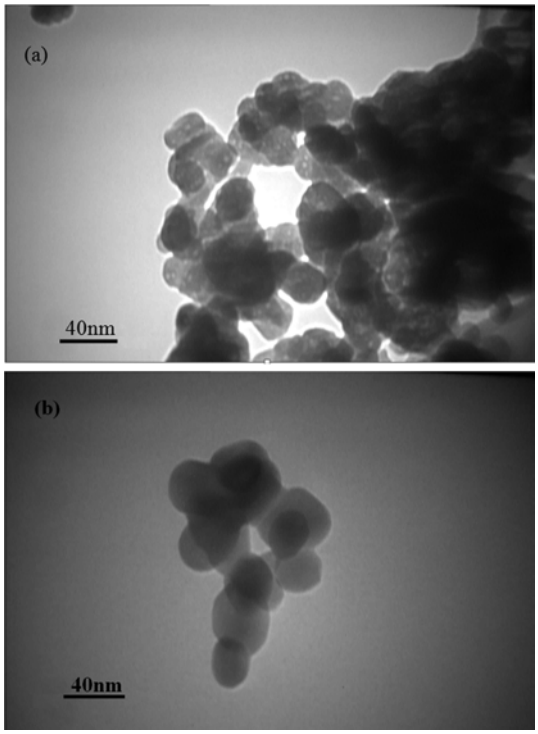

Fig. 6. TEM images of: (a) HA nanoparticles and (b) FA nanoparticles.

noticed that both of the nanopowders have a tendency to aggregate.

TEM analysis

TEM was used to examine and estimate the HA and FA crystallites. Fig. 6a and b show TEM images of HA and FA nanopowders. The figures indicate that both of the samples were prepared in nearly spherical and semi spherical granules with a smooth geometry and their sizes do not exceed 60 nm, confirming the SEM findings. It was also noticed that the particles have a tendency to agglomerate, specially with the HA nanoparticles, as shown in both figures.

Conclusions

Nanocrystalline HA and FA were synthesized via an ultrasonic irradiation method. According to the results, it was found that by using high-energy ultrasonic waves, both HA and FA were synthesized with a median size of approximately 45 nm. It was also noticed that the particles formed with a spherical and semispherical morphology. The analysis also indicated that the samples are formed with low levels of impurities. Also it was revealed the nanoparticles are formed as highly crystalline bioceramics.

References

1. A.R. Moshaverinia, S. Ansari, M. Moshaverinia b, N. Roohpour, J.A. Darr and I. Rehman, Acta Biomater 4 [1] (2008) 432-440.
2. H. WonKim, Y. MinKong, C. JunBae, Y. JungNoh and H. EeKim, Biomater, 25 [3] (2004) 2919-2926.
3. J. Sang Choa, Y. Na Koa, H. Young Kooa, M. Jong LEEb and Y. Chan KANGa, J. Ceram Pro. Resear. 10 [5] (2009) 628-632.
4. Y. Cai, P. Liu and R. Tang, Recent Patents on Materials Science 1 (2008) 209-216.
5. Laurence C. Chow and L. Sun, B. Hockey, J. Res. Natl. Inst. St and. Technol 109 [2] (2004) 543-551.
6. N. monmaturapoj and J. Metals, Mater and Min. 18 [1] (2008) 15-20.
7. A. Beganskienë, O. Dudko, R. Sirutkaitis and R. Giraitis, MATER SCIE. 9 [4] (2003) 383-386.
8. C.V. azquez, C.P. Barba and N. Mungu, REVIST. 51 [3] (2005) 284-293.
9. U. Vijayalakshmi, S. Rajeswari and Trends. Biomater. Artif. Organ, 19 [2], (2006) 57-62.
10. H. Eslami, M. Solati-Hashjin and M. Tahriri, Iran. J. Pharma. Sci. 4 [2] (2008) 127-134.
11. S. Bose and S.K. Saha, Chem. Mater. 15 [6] (2003) 4464-4469.
12. B. Nasiri, P. Honarmandi, R. Ebrahimi and P. Honarmandi, Mater. Let. 63 [2] (2009) 543-546.
13. K.C.B. Yeong, J. Wang, and S.C. Ng, Biomater 22 [1] (2001) 2705-2712.
14. C.C. Silva, A.G. Pinheiro, M.A.R. Miranda, J.C. Goes and A.S.B. Sombra, Solid State Sci. 5 [5] (2003) 553-558.
15. M. Shirkhanzadeh, J. Mater. Sci. Mater. Med. 9 [2] (1998) 67-72.
16. M. Sadat-Shojai, J. Iran. Chem. Soc. 6 [2] (2009) 386-392.
17. L. Montazeri, J. Javadpour, M.A. Shokrgozar, S. Bonakdar and S. Javadian, Biomed. Mater. 5 [3] (2010) 7-14.
18. A. Hassanjani-Roshana, M. Vaezi, A. Shokuhfar, Z. Rajabali, Particuo. 9 [1] (2011) 95-99.
19. M. Ashokkumar, J. Lee, S. Kentish and F. Grieser, ultra. sonochem. 14 [4] (2007) 470-475.
20. X.K. Wang, G.H. Chen and W.L. Guo, Molecu. 8 [2] (2003) 40-44.
21. T.J. Mason and J.P. Lorimer, "Applied Sonochemistry" (Wiley, VCH, Weinheim, 2002).
22. B. Avvaru and A. Pandit, Ultra. Sonochem. 15 [4] (2008) 578-589.
23. Philips MJ, PhD thesis, Queen Mary, University of London; (2005).
24. A. Balamurugan, J. Michel, J. Fauré, H. Benhayoune, L. Wortham, G. Sockalingum, V. Banchet, S. Bouthor, D. Laurent-Maquin and G. Balossier, Ceramics-Silikáty 50 [1] (2006) 27-31.